VELOCITY AND TEMPERATURE FLUCTUATIONS AND THEIR CORRELATIONS FOR TURBULENT AIR FLOW IN A TUBE

M. Kh. Ibragimov, V. I. Subbotin, and G. S. Taranov

UDC 532.517.4

The average fields and statistical characteristics of velocity and temperature fluctuations in a turbulent air flow have been measured at Reynolds numbers of 260,000 and 32,500. The correlation coefficients between the fluctuation components are determined, along with the distribution of the turbulent Prandtl number over the flow cross section.

Investigations of the statistical characteristics of turbulent fluid flow in ducts are normally confined to measurements of either the velocity fluctuations associated with isothermal flow or the temperature fluctuations under heat-transfer conditions. The study of the turbulent heat-transfer mechanism also requires simultaneous measurement of the velocity and temperature fluctuations in nonisothermal flow. This operation makes it possible to determine the correlation moments $\overline{ut}$ and $\overline{vt}$ and to compute the turbulent heat-transfer directly. We now present the results of such measurements.

Our investigation was carried out in a stabilized air flow in a smooth vertical tube having an inside diameter d = 113 mm and length $l \simeq 7$ m ($l/d \simeq 61$). An electric heater extended along the tube wall for a length equal to 35 d. The hydrodynamic regimes corresponded to Reynolds numbers of 32,500 and 260,000. The specific heat fluxes at these Reynolds numbers were 0.142 and 1.09 kW/m^2, and the temperature drops ($\theta_w - \theta_0$) were 8.2 and 13°C, respectively. The measurements were performed in the tube at distances of 50 mm (for isothermal flow) and 270 mm (for nonisothermal flow) from the exit section.

The turbulent velocity and temperature fluctuations were measured with a thermoanemometer operating on the principle of a dc heat filament. The probe was either a single-straight-filament or double-crossed-filament element made of tungsten wire, d = 5 μ, in a copper sheath, d = 40 μ. The sensitive part of the probe was formed by etching of the copper sheath over a length of 1.05 to 1.1 mm. During calibrations the probe filaments were oriented either perpendicular to the direction of air flow (straight probe) or at angles of 45 and 135° (crossed-filament probe).

The following procedure was used to measure the fluctuation components and correlation moments.

The longitudinal velocity and temperature fluctuations were determined by means of the direct probe with the filament oriented perpendicular to the flow direction. The velocity fluctuations in isothermal flow were measured with the filament heated 150 to 300°C above the ambient gas temperature, and the temperature fluctuations were measured with a small heating current through the probe filament (I_p = 3 to 7 mA), so that the probe would operate in the resistance thermometer mode.

In order to separate the radial and tangential components of the velocity fluctuations we used a crossed-filament probe with its mutually perpendicular filaments oriented symmetrically with respect to the average-velocity vector. The voltage fluctuations on the filaments when the latter are situated in the plane formed by the fluctuation velocity components u and v (plane xor) can be written as follows (see, e.g., [1]):

$$e_1 = -a_1 u - a_1 v, \quad (1)$$

$$e_2 = -a_2 u + a_2 v. \quad (2)$$

Translated from Inzhenerno-Fizicheskii Zhurnal, Vol. 19, No. 6, pp. 1060-1069, December, 1970. Original article submitted December 29, 1969.

The conventional technique for separating the component v [1] is to subtract the filament signals for identical filaments. In this case $a_1 = a_2 = a$, and the signal difference is proportional to the component v:

$$e_2 - e_1 = 2av.$$

The fabrication of a crossed-filament probe having identical filaments is exceedingly complicated in practice. With our etching technology the lengths of the sensitive parts of the filaments differed at most by 0.02 mm (2%). The disparity of the filament sensitivities for the same degree of overheating, on the other hand, was generally higher.

However, it is not necessary for the probe elements to be strictly identical. For the given measurements the filament sensitivities were made almost identical by the proper choice of overheating, i.e., the overheating of one filament was varied so as to equalize the sensitivity of that filament with the sensitivity of the other. Under this condition the signal disparity is also proportional to the transverse component.

The overheating values were monitored on the basis of the fact that when they are properly chosen the root mean square signal amplitudes from each filament are zero on the tube axis, while in the case of measurement of the component w, when the filaments are situated in the plane $xo\varphi$, they are equal at all other points.

It was assumed in the measurements that the time constants of the filaments were equal due to the proximity of their parameters and that the difference of the signals, rather than the signal from each filament separately, was delivered to the thermal lag compensation circuit of the probes.

The separation of the probe signals corresponding to the components v and w was realized mainly in their spectral analysis and recording of the oscillograms. The determination of the correlation moment $\overline{uv}$ and the intensities $\overline{\sigma}_v$ and $\overline{\sigma}_w$ does not require adjustment of the sensitivities, and the measurements can be performed at the calibration overheating values for the filaments. Thus, the variances of signals (1) and (2) may be written

$$\overline{e_1^2} = a_1^2(\overline{u^2} + \overline{v^2} + 2\overline{uv}), \tag{3}$$

$$e_2^2 = a_2^2(\overline{u^2} + \overline{v^2} - 2\overline{uv}). \tag{4}$$

Then

$$\overline{uv} = \frac{1}{4}\left(\frac{\overline{e_1^2}}{a_1^2} - \frac{\overline{e_2^2}}{a_2^2}\right), \tag{5}$$

$$\overline{v^2} = \frac{1}{2}\left(\frac{e_1^2}{a_1^2} + \frac{e_2^2}{a_2^2}\right) - \overline{u^2}. \tag{6}$$

For the calculation of σ_v from (6) we used the values of $\sigma_u^2 = \overline{u^2}$ determined by the straight probe.

A similar technique was used to determine the tangential fluctuation intensity at Re = 260,000. The intensity σ_w at Re = 32,500 was measured directly from the signal difference from the filaments of the obliquely oriented probe.

Special measurements showed that for the low thermal flux density present in the experiments the velocity fluctuation intensities and value of the correlation moment $\overline{uv}$ are practically equal for both isothermal and nonisothermal air flows.

The single-point correlation moment $\overline{ut}$ was measured with a straight probe. In nonisothermal flow the filament voltage fluctuation and its variance can be represented by the expressions

$$e = -au + bt, \tag{7}$$

$$\overline{e^2} = \underset{\text{I}}{a^2\overline{u^2}} + \underset{\text{II}}{b^2\overline{t^2}} - \underset{\text{III}}{2ab\overline{ut}}. \tag{8}$$

It is clear that the correlation moment must be measured for overheating values sufficient to achieve the maximum weight of $\overline{ut}$ in the signal variance. It can be shown that this condition is satisfied by maximization of the ratio

$$f\left(\frac{b}{a}\right)=\frac{\left|2\frac{b}{a}\overline{ut}\right|}{\left|\overline{u^2}+\frac{b^2}{a^2}\overline{t^2}-2\frac{b}{a}\overline{ut}\right|},$$

which is a maximum for $b/a = \sigma_u/\sigma_t$.

The function $f(b/a)$ does not have a sharp maximum, thus making it possible to vary the ratio b/a without significantly diminishing the relative weight of $\overline{ut}$. For the indicated numbers Re the overheating values of the filaments were chosen so as to vary the ratio b/a from 0.5 to 4 m/sec/deg.

The measurements were carried out in the following sequence.

1) The variance of the signal (8) was determined in nonisothermal flow for three or four overheating values corresponding to different values of the heating current I_w and filament resistance R_w.

2) For low heating, I_g = 3 to 6 mA (resistance R_g), the temperature fluctuation intensity σ_t was determined.

Inasmuch as the temperature sensitivity of the filament can be represented by the relation [1]

$$b = I\beta R_0\frac{R_w}{R_g},$$

the second term (II) of expression (8) can be calculated from the signal variance obtained for a low current I_g:

$$b^2\overline{t^2}=\sigma_t^2\left(\frac{I_w}{I_g}\cdot\frac{R_w}{R_g}\right)^2;$$

3) The contribution of longitudinal velocity fluctuations to the signal variance, i.e., the first term $a^2\overline{u^2}$ of expression (8), was determined in isothermal flow at the air velocities and filament sensitivities a corresponding to part 1).

It follows from (8) that the correlation coefficient is

$$R_{ut}=\frac{\overline{e^2}-a^2\overline{u^2}-b^2\overline{t^2}}{2\left(a^2\overline{u^2}\cdot b^2\overline{t^2}\right)^{0.5}}.$$

The arithmetic-mean value for all overheating values chosen in part 1) was adopted as the resultant value of R_{ut}.

The turbulent heat flux density in the axial direction is then written as follows:

$$q_x=\rho c_p\overline{ut}=\rho c_p R_{ut}\sigma_u\sigma_t.$$

This method of determining the correlation of u and t does not require precise knowledge of the sensitivities of the probe to velocity and temperature fluctuations. This feature eliminates the error in the determination of R_{ut} due to errors in the determination of the probe characteristics. It is required, however, that all the measurements be carried out with the same probe. Earlier [2] in the flow regime Re = 32,500 the coefficient R_{ut} was determined from the average value of the correlation moment calculated on the basis of measurements with different probes. The determination of R_{ut} was then repeated by the procedure described here. In the central part of the tube ($2r/d$ = 0 to 0.3), where $\overline{ut}$ is relatively small and is therefore more sensitive to measurement errors, as a result, the values of R_{ut} obtained by this method proved to be somewhat lower than in [2]. In the rest of the flow domain both measurement cycles yielded satisfactory agreement.

The correlation moment $\overline{vt}$, which characterizes the radial heat flux density, was determined with crossed-filament probes. By analogy with (1) and (2), the filament signals in nonisothermal flow can be represented by the expressions

$$e_1=-a_1u-a_1v+b_1t, \tag{1a}$$

$$e_2=-a_2u+a_2v+b_2t. \tag{2a}$$

Hence the difference between the variances is

$$\overline{e_1^2} - \overline{e_2^2} = (a_1^2 - a_2^2)\,\overline{u^2} + (a_1^2 - a_2^2)\,\overline{v^2} + (b_1^2 - b_2^2)\,\overline{t^2} + 2(a_1^2 + a_2^2)\,\overline{uv} - 2(a_1b_1 - a_2b_2)\,\overline{ut} - 2(a_1b_1 + a_2b_2)\,\overline{vt}.$$

The identity of the filaments greatly simplifies the measurement of the correlation moments. This case has been analyzed in detail in [1]. For $a_1 = a_2 = a$ and $b_1 = b_2 = b$ the difference of the variances is determined by the correlation moments $\overline{uv}$ and $\overline{vt}$, and for their determination it is sufficient to perform the measurements at two filament overheating levels:

$$\overline{e_1^2} - \overline{e_2^2} = 4a^2\overline{uv} - 4ab\overline{vt}.$$

However, strict identity of the filaments is not observed in practice. Nevertheless, the influence of the disparity in the filament sensitivities can be eliminated by the proper choice of the overheating level. In the measurements the resistances of the heated filaments were chosen so as to equalize the ratios of the velocity and temperature coefficients, i.e., to make

$$\frac{b_1}{a_1} = \frac{b_2}{a_2} = \frac{b}{a}.$$

In this case also there is mutual compensation of the variances of the velocity and temperature fluctuations and correlation moment $\overline{ut}$:

$$\frac{\overline{e_1^2}}{a_1^2} - \frac{\overline{e_2^2}}{a_2^2} = 4\left(\overline{uv} - \frac{b}{a}\,\overline{vt}\right),$$
$$\overline{vt} = \frac{a}{b}\left[\frac{1}{4}\left(\frac{\overline{e_2^2}}{a_2^2} - \frac{\overline{e_1^2}}{a_1^2}\right) + \overline{uv}\right]. \qquad (9)$$

By the proper choice of the filament overheating levels it is possible to obtain two independent equations for the calculation of the correlation moments.

As in the determination of $\overline{ut}$, the filament overheating levels can be chosen to satisfy the condition that the weight of $\overline{vt}$ in the signal variance be close to the maximum. This requirement is met for

$$\frac{b}{a} = \left(\frac{\overline{u^2} + \overline{v^2} \pm 2\overline{uv})}{\overline{t^2}}\right)^{0.5}. \qquad (10)$$

In order to increase the accuracy of the results the measurements were performed at three or four temperature levels close to condition (10). The correlation moment $\overline{vt}$ was calculated according to (9), where the value of $\overline{uv}$ was assumed to be equal to its values for isothermal flow. The correlation coefficient was determined from the relation

$$R_{vt} = \frac{\overline{vt}}{\sigma_v\sigma_t}.$$

Under the experimental conditions the probe filaments had a time constant of $3 \cdot 10^{-4}$ to $7 \cdot 10^{-4}$ sec. The influence of thermal lag on the measurements was compensated with an RC section inserted between the probe signal amplification stages I and II.

An amplifier having a regulatable pass band was used for stage I. The lower limit of the band corresponds to a frequency of 0.18 Hz, and the upper limits to 30, 300, and 1000 Hz. The amplifier input circuit had a built-in capability for noise amplitude and phase balancing; the internal noise of the amplifier, referred to the input conditions, did not exceed 2 microvolts. The second stage was a U-4 amplifier.

At low Reynolds numbers the frequency band of the amplifiers corresponded to the energy spectrum of the turbulent fluctuations. An analysis of the signal spectrum at Re = 260,000 showed that the possible error due to the finite bandwidth of the instruments is $\approx 8\%$.

The amplifier probe signals were recorded on a loop oscillograph or were delivered to a correlometer, which determined the root mean square signal amplitude or its variance. The correlometer [3] had a regulatable integration time interval from 1 to 5 min.

The average-velocity distribution in the tube was determined with a total-head manometer, and the average temperature with a thermocouple having a junction diameter of 0.2 mm. The velocity and temperature fields for one given Re number coincide in a large portion of the flow (2r/d = 0 to 0.8) (Fig. 1).

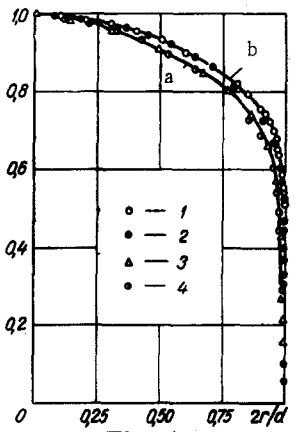

Fig. 1

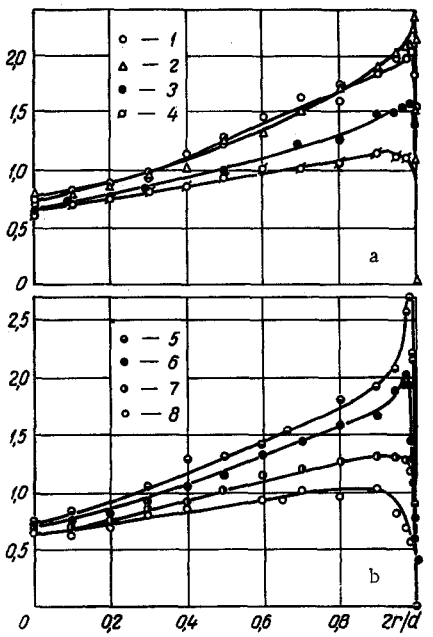

Fig. 2

Fig. 1. Average-velocity and temperature fields. a) Re = 32,500; b) Re = 260,000; 1, 3) U/U_0; 2,4) $(\theta_w - \theta)/(\theta_w - \theta_0)$.

Fig. 2. Turbulent velocity and temperature fluctuations in the tube. a) Re = 260,000: 1) σ_t/t^*Pr; 2) σ_u/u_τ; 3) σ_w/u_τ; 4) σ_v/u_τ; b) Re = 32,500: 5) σ_u/u_τ; 6) σ_t/t^*Pr; 7) σ_w/u_τ; 8) σ_v/u_τ.

The relative intensities of the temperature fluctuations and the three components of the fluctuation velocity are given in Fig. 2. The turbulent fluctuation intensities increase from the axis toward the tube wall. The disparity between σ_u, σ_v, and σ_w increases in the same direction, indicating an increase in the flow anisotropy. The degree of flow anisotropy for Re = 260,000 in this case is lower than for Re = 32,500.

The intensities of the longitudinal velocity and temperature fluctuations, plotted as σ_u/u_τ and σ_t/t^*Pr, have the same behavior over the flow cross section, and for Re = 260,000, excluding the wall region, they practically coincide.

The velocity and temperature fluctuations have maximum intensities at distances very close to the wall. Thus, for Re = 32,500 the values of σ_u and σ_t are a maximum at $y^+ = 13$ and $y^+ = 19$, respectively, i.e., near the maximum turbulence energy. The temperature fluctuation intensity maximum in this case is far from the wall, probably because of the large thickness of the molecular thermal-conduction substrate relative to the viscous substrate.

The measured velocity fluctuation intensities are highly consistent with the results of [4], and the temperature fluctuation intensities (Re = 32,500) correspond to the data of [5] obtained for air flowing in a tube at Re = 39,000.

In the flow core the shear stresses ($\rho\overline{uv}$) referred to the frictional stress at the wall (ρu_τ^2) provide a good fit to a straight line and are close to the total stress (Fig. 3). For Re = 260,000 this quantity is somewhat below the total stress values. The indicated discrepancy (about 2.5%) does not exceed the measurement error (5 to 8%) due to the narrowness of the instrument signal pass band.

From the correlation moments $\overline{vt}$ and $\overline{ut}$, which determine the heat transfer by fluctuation motion, we calculated the heat flux densities in the radial ($q_r = \rho c_p \overline{vt}$) and axial ($q_x = \rho c_p \overline{ut} = \rho c_p R_{ut} \sigma_u \sigma_t$) directions (Fig. 3).

The relative turbulent heat flux density q_r/q_w in the radial direction approaches the stress line as the Re number is increased. The distribution of q_x/q_w is virtually independent of the Reynolds number. Over the entire cross section of the tube the heat flux density along the tube axis exceeds the flux density in the radial direction. The q_r/q_x tubes have maxima between the limits 0.65 to 0.7 for $2r/d \simeq 0.5$.

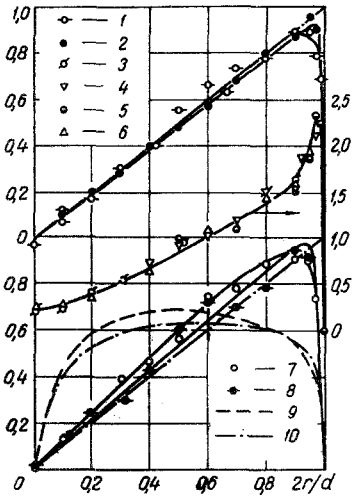

Fig. 3

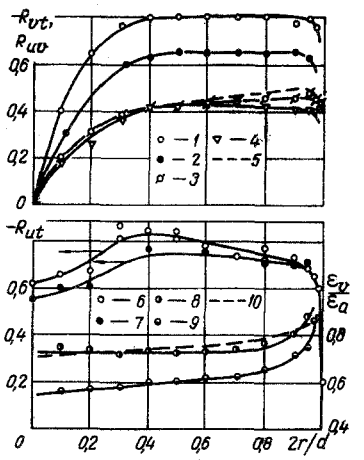

Fig. 4

Fig. 3. Turbulent shear stress and heat flux distributions over the tube radius. 1) $\overline{uv}/u_\tau^2$, Re = 32,500; 2) $\overline{uv}/u_\tau^2$, Re = 260,000; 3, 4, 5) q_x/q_w, Re = 32,500; 6) q_x/q_w, Re = 260,000; 7) q_r/q_w, Re = 32,500; 8) q_r/q_w, Re = 260,000; 9) q_r/q_x, Re = 32,500; 10) q_r/q_x, Re = 260,000.

Fig. 4. Distributions of the correlation coefficients and turbulent Prandtl number for air flow in a tube. 1) R_{vt}, Re = 32,500; 2) R_{vt}, Re = 260,000; 3) R_{uv}, Re = 32,500; 4) R_{uv}, Re = 260,000; 5) R_{uv} from [4]; 6) R_{ut}, Re = 32,500; 7) R_{ut}, Re = 260,000; 8) Pr_T, Re = 32,500; 10) Pr_T from [11].

The measured values of the correlation moments and fluctuation intensities were used to calculate the single-point correlation coefficients both between the fluctuation velocity components (R_{uv}) and between the velocity and temperature fluctuations (R_{vt}). The symmetry of the average velocity and temperature fields causes the coefficients R_{uv} and R_{vt} to be equal to zero on the flow axis (Fig. 4), whereas the correlation of the longitudinal velocity fluctuation with the temperature fluctuations is high ($R_{ut} \approx -0.6$).

On moving further away from the tube axis, the correlation coefficients R_{uv} and R_{vt} increase with the average field gradients and, beginning with $2r/d > 0.4$, assume values that remain almost constant up to the wall region. The quantity R_{vt} in this case is one and a half to two times R_{uv} (in absolute value).

At distances $2r/d > 0.95$ the correlation of the velocity and temperature fluctuations falls off. The tube wall upsets the statistical correlation between them: for $2r/d = 1$ the velocity fluctuations are equal to zero, whereas the temperature fluctuations penetrate the wall [6]. Clearly, R_{vt} and R_{ut} become equal to zero at the wall.

Moreover, the tube wall limits the turbulent disturbance primarily in the transverse, rather than the longitudinal, direction. Consequently, near the wall ($2r/d > 0.95$) the correlation of the transverse and longitudinal velocity fluctuations also begins to weaken.

The values obtained for R_{uv} are in good agreement with the measurements of [4].

If we formally introduce the turbulent viscosity and thermal conductivity coefficients according to the Bussinesq principle, we can express the turbulent Prandtl number as follows in terms of the correlation moments and average flow characteristics:

$$-\overline{uv} = \varepsilon_v \frac{dU}{dr}, \tag{11}$$

$$-\overline{vt} = \varepsilon_a \frac{d\theta}{dr}, \tag{12}$$

$$Pr_T = \frac{\varepsilon_v}{\varepsilon_a} = \frac{\overline{uv}}{\overline{vt}} \cdot \frac{d\theta}{dU}.$$

The experiment showed that the dimensionless velocity and temperature fields in the flow region $2r/d < 0.8$ practically coincide, so that

$$Pr_T = \frac{\overline{uv}}{\overline{vt}} \cdot \frac{\theta_0 - \theta_w}{U_0}.$$

The number Pr_T for $2r/d > 0.8$ was calculated with a correction for the inconsistency of the velocity and temperature profiles. The correction introduced here turned out to be inconsequential and did not induce any appreciable variations in the behavior of the dependence of Pr_T on $2r/d$.

The turbulent Prandtl number is less than unity over the entire flow cross section (Fig. 4). In the central region of the tube the value of Pr_T varies only slightly and may be assumed constant for each value of Re.

According to the measurement results in the present study, Pr_T increases with Re. The tendency of Pr_T to increase (without exceeding unity) with Re for an air flow in a duct has also been noted in the experimental studies [7, 8], in which Pr_T was determined by the gradient method without a measurement of the correlation moments $\overline{uv}$ and $\overline{vt}$. A theoretical calculation of Pr_T on the basis of a modified Prandtl hypothesis concerning the displacement length [9] also predicts an increase in Pr_T with an increase in the Reynolds number.

It is possible that the indicated behavior of Pr_T reflects the dominant contribution of anisotropic large-scale turbulence to the heat transfer, rather than to the momentum-transfer, process.

Thus, expressions (11) and (12) are for the most part of a formal character. They are valid as long as the transfer of heat and momentum are caused in equal degree by gradient-type diffusion.

As mentioned in [1, 10], the heat transfer in a free turbulent shear flow has a mixed character and is determined by gradient-type diffusion for small-scale turbulence and by volume convection created by large-scale turbulent disturbances. It is obvious that the same mechanism is present in the case of wall turbulence in a duct.

Accordingly, if we denote by v the part of the fluctuation velocity due to large-scale motion, and by ε_a^{gr} the thermal diffusivity due to small-scale motion, we can write

$$-\overline{vt} = \varepsilon_a^{gr} \frac{d\theta}{dr} - \overline{\tilde{v}\tilde{t}}. \tag{13}$$

We infer from a comparison of (12) and (13) that

$$\varepsilon_a = \varepsilon_a^{gr} \left(1 - \frac{\overline{\tilde{v}\tilde{t}}}{d\theta/dr} \right),$$

i.e., ε_a calculated according to (12) includes both the gradient and the large-scale transfer effects.

With an increase in Re the flow tends to become isotropic, causing a decrease in the fraction of heat transfer due to the anisotropic large-scale component. This fact brings the coefficients ε_a and ε_ν closer together.

Similarly, the flow structural variations that tend to diminish the role of the anisotropic large-scale turbulence component cause the statistical correlation between the velocity and temperature fluctuations to diminish and R_{vt} to approach R_{uv} in absolute value as Re is increased (Fig. 4).

The values of Pr_T increase with distance from the tube axis ($2r/d > 0.8$), an effect that is also apparently elicited by the increase in the small-scale transfer intensity as the average-field gradients increase and the scales of the velocity and temperature perturbations in the wall region decrease.

Earlier calculations of the turbulent Prandtl number for an air flow on the basis of the velocity and temperature fields [7, 8, 11, 12] indicate both an increase in its values as the wall is approached, according to some authors, and a decrease according to others. The best correspondence in the behavior of Pr_T over the tube cross section exists between the results obtained here and the data of [11].

NOTATION

d, r, l are the diameter, radius, and length of the tube;
oxrφ is the cylindrical coordinate system;

ox	is the direction of the tube axis;
or	is the radial direction;
$o\varphi$	is the tangential direction;
y	is the distance from the wall;
U_0	is the velocity on the flow axis;
U	is the average local velocity;
u_τ	is the dynamic velocity;
θ_w, θ, θ_0	are the wall temperature, local temperature, and air temperature on the flow axis;
u, v, w	are the longitudinal, radial, and tangential components of the fluctuation velocity;
t	is the temperature fluctuation;
σ_u, σ_v, σ_w, σ_t	are the intensities of the fluctuation velocity components and temperature fluctuation;
$\overline{uv}$, $\overline{ut}$, $\overline{vt}$	are the correlation moments between the corresponding fluctuation variables;
R_{uv}, R_{ut}, R_{vt}	are the correlation coefficients between the corresponding fluctuation variables;
c_p, ρ, ν	are the specific heat, gas density, and kinematic viscosity;
q_w	is the heat flux density at the wall;
$q_x = c_p\rho\overline{ut}$, $q_r = c_p\rho\overline{vt}$	are the turbulent heat flux densities along the tube axis and along the radius;
R_0, R_g, R_w	are the resistance of the thermoanemometer filament at 0°C, local temperature of the gas, and local temperature of the overheated filament;
β	is the temperature coefficient of the resistance;
I_g	is the low current ensuring operation of the filament as a resistance thermometer;
I_w	is the filament heating current;
a, b	are the probe sensitivity to velocity and temperature fluctuations, respectively;
e	is the instantaneous values of the probe filament voltages;
Re	is the Reynolds number;
Pr	is the Prandtl number;
ε_ν, ε_a, $Pr_T = \varepsilon_\nu/\varepsilon_a$	are the turbulent viscosity, thermal diffusivity, and turbulent Prandtl number;
$t^* = q_w/c_p\rho u_\tau$;	
$y^+ = yu_\tau/\nu$.	

LITERATURE CITED

1. J. O. Hinze, Turbulence, McGraw–Hill, New York (1959).
2. M. Kh. Ibragimov, V. I. Subbotin, and G. S. Taranov, Dokl. Akad. Nauk SSSR, 183, No. 5 (1968).
3. V. P. Bobkov, Yu. I. Gribanov, M. Kh. Ibragimov, E. V. Nomofilov, and V. I. Subbotin, Teplofiz. Vys. Temp., 3, No. 5 (1965).
4. J. Laufer, NACA Rep. No. 1174 (1954).
5. S. Tanimoto and J. Hanratty, Chem. Engng. Sci., 18, 5 (1963).
6. V. I. Subbotin, M. Kh. Ibragimov, and E. V. Nomofilov, Teploénergetika, No. 3 (1962).
7. C. A. Sleicher, Trans. ASME, 80, 3 (1958).
8. F. Page, W. C. Schlinger, D. K. Breaux, and B. H. Sage, Ind. Engng. Chem., 44, 424–430 (1952).
9. H. Z. Azer and B. T. Chao, Internat. J. Heat and Mass Transfer, 1, 121–138 (1960).
10. A. A. Townsend, The Structure of Turbulent Shear Flow, Cambridge Univ. Press (1956).
11. R. A. Gowen and I. W. Smith, Internat. J. Heat and Mass Transfer, 11, 11 (1968).
12. H. Lundwieg, Z. Flugwissensch., 4, Nos. 1/2 (1956).